

Interactive Deformation Simulation of Manual Girth Measurement for Limbs

Jianhui Zhao*, Yihua Ding*, Ravindra S. Goonetilleke**, Shuping Xiong***
Yuanyuan Zhang*, Chengjiang Long*, Zhiyong Yuan*

**Computer School, Wuhan University, Wuhan, Hubei, 430072, PR China
E-mail: jianhuizhao@whu.edu.cn*

***Department of Industrial Engineering and Logistics Management, Hong Kong University of Science and Technology, Hong Kong*

****School of Design and Human Engineering, Ulsan National Institute of Science and Technology, Ulsan, 689-798, Republic of Korea*

Abstract

The existing methods for automatic girth measurement are primarily based on 3D point cloud or its generated surfaces, without considering limbs' elasticity and thus the interactive deformation during manual measurement. Taking human foot as example, we propose a new method to simulate manual girth measurement using 3D triangular mesh and mass-spring model. The deformation is limited in the local deformed region consisted of tape region, propagation region and compensation region, while the latter two regions are controlled with depth parameters representing the affected ranges of limb surface from external forces. We also present a novel algorithm to dynamically calculate volume change of the deforming limb, and then repair the lost volume with compensation function. Our approach has the advantages of low computational complexity and realistic volume preserved simulation for interactive deformation in manual measurement. The proposed method is tested with experimental results, which illustrate its efficiency in many applications such as custom products making.

Keywords: Interactive deformation, Triangular mesh, Mass-spring model, Volume preservation

1. Introduction

Computer based approaches have achieved popularity in automatic measurement of human limbs, such as foot measurements in shoe manufacturing industry [1]. Up until now, different techniques have been designed to automatically obtain the dimensions. Compared with linear measurements, girth dimensions are more difficult to determine as the digitized points are only discrete samples of the continuous real surface. Xu et al. [2] constructed triangular meshes from unorganized point cloud, generated continuous multiple lines, and calculated the girth as sum of all lengths. Witana et al. [3] projected 3D scanned points nearby the plane of measurement onto one 2D plane, and then used convex hull of projected points to compute the girth. Zhao et al. [4] used Non-Uniform Rational B-Spline (NURBS) to generate smooth surface from 3D points, then the intersected curve between NURBS surface and tape plane

was taken as the simulated girth. All of the above methods are performed on the limb kept still in its certain posture. However, interactive deformation between tape and limb exists in realistic manual girth measuring, and such a fact introduces the deviations between automatic and manual measurements for girth dimensions. Therefore, it is necessary to develop a novel method to simulate manual girth measurement considering limb deformation.

Recently, deformation simulation has become an important topic in computer graphics and virtual reality, and physically based deformation models are generally utilized to reach the realistic visual effect. Oomens et al. [5] simulated human skin deformation with finite element method, although realistic and visually convincing results can be produced, it is inappropriate to achieve real-time use or interaction [6] due to the shortcoming of expensive computational cost. De et al. [7] proposed the point-associated finite field approach based upon the equations of motion dictated by physics. Nonetheless, the same defect is the high computational cost which cannot be overlooked. In contrast, mass-spring model [8] is widely used in deformation simulation of elastic objects owing to its simplicity and low computing complexity. Although mass-spring model is a feasible method to simulate limb deformation, the existing methods still have difficulties to achieve accurate volume preservation [9].

In this paper, we propose one mass-spring model based method for real time deformation simulation of manual measurement with more accurate volume preserving. The rest of our paper is organized as follows: related definitions are presented in Section 2, the deformation simulation algorithm is proposed in Section 3, the volume preservation algorithm is proposed in Section 4, experiments are analyzed in Section 5, and conclusion is given in Section 6.

2. Related Definitions

The following definitions are used in our approach for interactive deformation simulation.

(1) Deformation region: the limb region that the tape covers and affects, comprising the tape region, the propagation region and the compensation region;

(2) Tape region: the region that the tape covers, namely, the region including all the points which are directly imposed by external forces from the tape;

(3) Propagation region: the deformation region that is triggered by the external forces, but except for the tape region;

(4) Compensation region: the region where the compensation function works in order to compensate the volume loss during deformation;

(5) Propagation depth: the parameter to control the region range where the external forces indirectly affect in the deformation model;

(6) Compensation depth: the parameter defined in the compensation function, which is used to adjust the scope of volume compensation.

3. Deformation Simulation Based on Mass-spring Model

3.1 Control of local deformation

In general the mass-spring model works on the whole limb, and it is not necessary to control the deformation range. But in our study the deformation only occurs in the deformed region during the procedure of manual girth measurement. Therefore, we define propagation depth of the external force, as shown in Fig. 1.

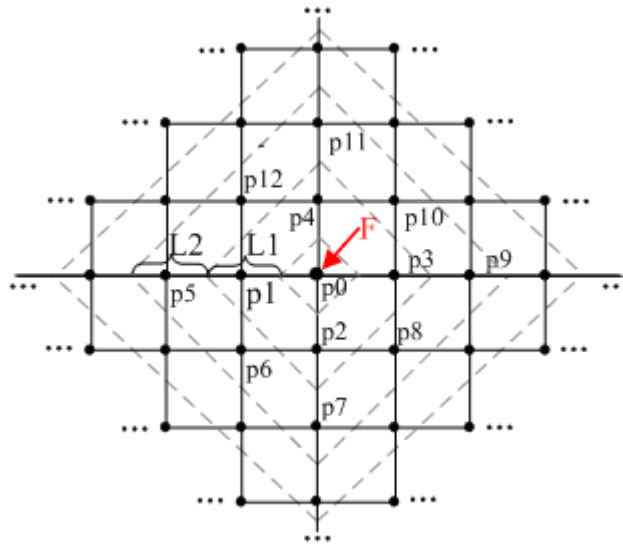


Fig. 1. Interaction in the planar lattice.

When mass p_0 is imposed with an external force F , p_0 is moved and the elastic force is generated from other masses connected with p_0 . As a result, the external force transfers to all masses in the next layer L_1 of p_0 , i.e. p_1, p_2, p_3 and p_4 . Then mass p_1 is moved by the elastic force of its adjacent points. Similarly, as masses in layer L_1 are connected with those of layer L_2 , the force is transferred to 8 masses of layer L_2 , i.e. masses $p_5 \sim p_{12}$. Through changing the value of propagation depth, the number of deformation layers can be limited while the computational cost is controlled simultaneously. Of course, the local deformation control method can be applied on 3D models rather than the illustrated planar lattice.

3.2 Interaction of multiple external forces

Each mass covered by tape is imposed with the external force due to tape shrinkage, and all covered masses construct the tape region, i.e. region between two red lines in Fig. 2. All

external forces performing on tape region are so-called multiple external forces. Interaction of multiple external forces is implemented by transferring the forces from tape covered masses to the others orderly, during which the queue method is adopted as follows.

Step 1: Take the tape covered masses that contact with the multiple external forces directly as the head of the queue, and define their depth as zero.

Step 2: Apply breadth first search method to make sure that all masses in the deformation region enter the queue “from shallow to deep” [10], all the masses in the same layer have the equivalent priority, and the layers are searched and stored into the queue orderly.

Step 3: Stop searching after the propagation depth reaching the predefined value n , and then the queue is ready for further processing.

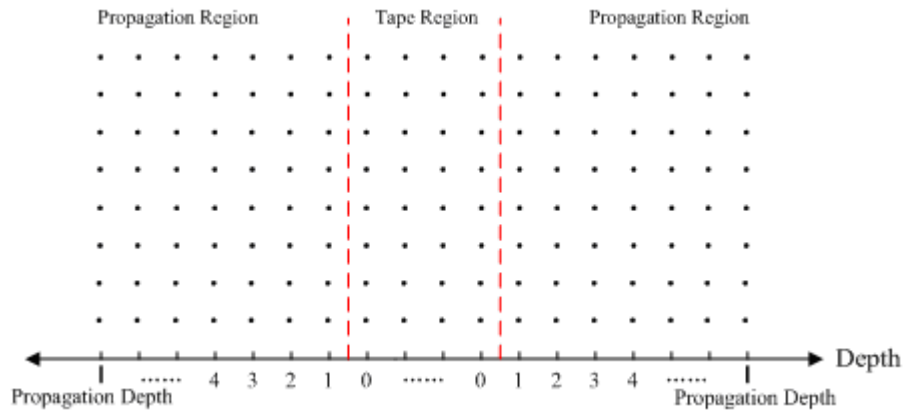


Fig. 2. Distribution of tape region and propagation region.

4. Volume Preserved Deformation

4.1 Calculation of volume change

In mass-spring system, the movements of all masses cause the deformation result. We can obtain the limb volume change at any moment by accumulating the unit change caused by the movement of each mass at that time. Take mass P and its neighboring masses P_1, P_2, \dots, P_n as one example, the movement from P to Q is illustrated in Fig. 3.

For the affected triangle $\Delta P_1 P_2 P$ with normal vector \vec{N} , when mass P moves to Q , the translation vector is \vec{PQ} and a tetrahedron $P_1 P_2 P Q$ is generated. Obviously, the volume of tetrahedron $P_1 P_2 P Q$ is the volume change ΔV triggered by triangle $\Delta P_1 P_2 P$ and the movement of mass P . The sign of ΔV is decided by the product of vector \vec{N} and vector \vec{PQ} . If $\vec{N} \cdot \vec{PQ} < 0$, $\Delta V = -V(P_1 P_2 P Q)$; if $\vec{N} \cdot \vec{PQ} > 0$, $\Delta V = V(P_1 P_2 P Q)$. In this way,

volume change of the whole limb can be obtained by accumulation of the volume changes caused by movements of all masses.

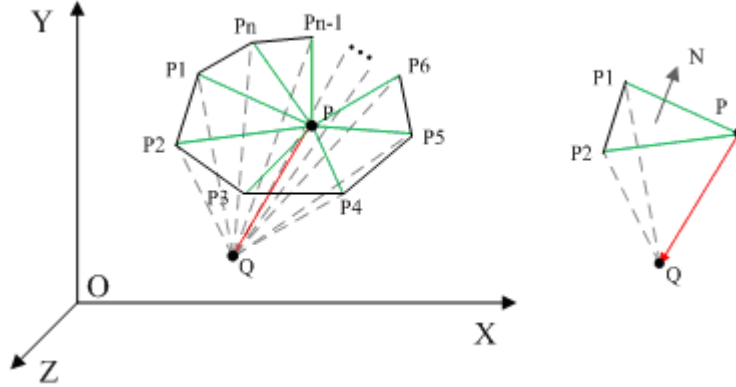


Fig. 3. Calculation of the volume change.

4.2 Function based volume compensation

To compensate the volume loss, we define the compensation region besides tape region and propagation region, and adopt the parameter of compensation depth to control the range of compensation region with the help of compensation function. Take 2D lattice for example, the distribution of deformation region on one side of the tape is shown in Fig. 4. Suppose the propagation depth is represented by $Depth_1$ and the compensation depth is represented by $Depth_2$, the compensation function is designed as

$$h_{i,j} = \begin{cases} A \cdot \sin\left(\frac{\pi}{2} \cdot \frac{i - Depth_1}{control - Depth_1}\right) & Depth_1 \leq i \leq control \\ \frac{A}{2} + \frac{A}{2} \cdot \cos\left(\pi \cdot \frac{i - control}{Depth_2 - control}\right) & control < i \leq Depth_2 \end{cases} \quad (1)$$

where $h_{i,j}$ is the compensation value of the j th mass in depth i , A is the amplitude of compensation function related to volume change because of deformation and the method to determine it will be mentioned below, $control$ is the controlling factor used to change the appearance of the compensation region.

For any mass $p_{i,j}$ in compensation region, $h_{i,j}$ can be obtained by Eq. (1) and new mass $p'_{i,j}$, i.e. the new position of mass $p_{i,j}$, can be obtained using Eq. (2), where $normal_{i,j}$ is the normal vector of mass $p_{i,j}$.

$$p'_{i,j} = p_{i,j} + \frac{normal_{i,j}}{|normal_{i,j}|} \cdot h_{i,j} \quad (2)$$

Suppose $\Delta v_{i,j}$ is the compensated volume caused by moving mass $p_{i,j}$ to mass $p'_{i,j}$, the compensation value of the whole model volume V_{sum} is computed as

$$V_{sum} = \sum_{j=0}^{i_{sum}} \sum_{i=Depth_1}^{Depth_2} \Delta v_{i,j} \quad (3)$$

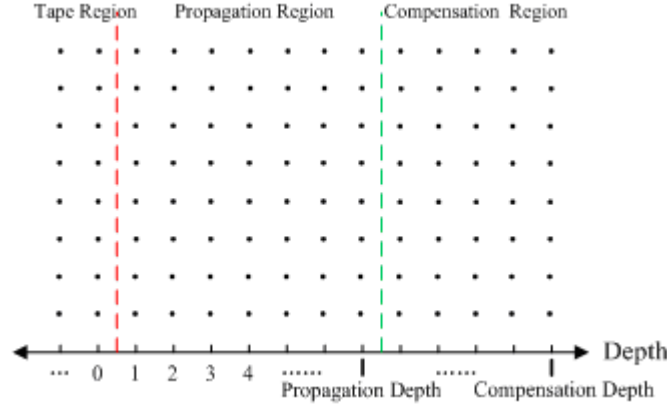


Fig. 4. Distribution of half deformation region.

Assume the volume change is V_{Change} and the volume loss after volume compensation is ΔV , there is $\Delta V = V_{sum} + V_{Change}$. Suppose the threshold value of ΔV is d and the iteration step length is $StepLen$, which is used to calculate the ultimate value of A in Eq. (1), then parameter A is determined in the following way:

Step 1. If $V_{Change} < 0$, set $StepLen$ less than zero in order to make sure $V_{sum} \geq 0$, while if $V_{Change} > 0$, set $StepLen$ more than zero to make $V_{sum} \leq 0$.

Step 2. If A makes $\Delta V < 0$, A is increased by $A = A + StepLen$, while if A makes $\Delta V > 0$, A is decreased by $A = A - \frac{1}{2} StepLen$; then $StepLen = \frac{1}{2} StepLen$.

Step 3. Repeat Step 2 until ΔV less than the predefined threshold value d , then stop.

Therefore, the way to determine the parameter A is also the iterative procedure to compensate the lost volume during limb deformation.

5. Experimental Results

Our algorithm is tested with simulation of interactive deformation for human foot. As shown in Fig. 5, the 1st row illustrates 3 foot models deformed after iteration of 5 times, 15 times, and 25 times respectively without volume compensation; while the 2nd

row displays the deformed results with volume compensation. Comparatively, our proposed volume preserved algorithm obtains more realistic deformation simulation.

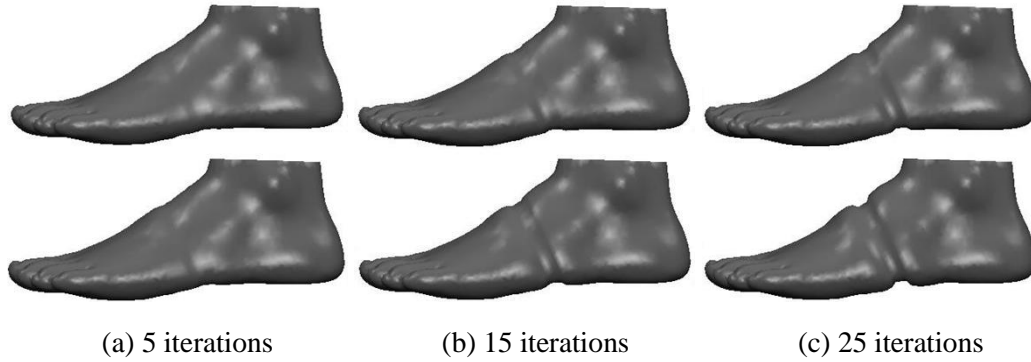


Fig. 5. Deformation simulation results on foot.

Experiment is also performed on simulated girth measurement with foot model. As listed in Table 1, results of two girth measurement methods [1] on deformed limbs with different iteration times are compared, and the deviations between two methods are presented. It can be found that our deformation approach has the capability to preserve limb's volume. It also unveils that the deviation (Girth value of Method 1 - Girth value of Method 2) decreases with the increase of iteration times, and the beneath reason is that the aperture between the tape and the limb becomes less with the more serious deformation, thus girth value of contacting along surface and girth value of stretching around surface tend to be identical.

Table 1. Results of girth measurement on deformed limb (Unit: mm).

Iteration times	Volume loss	Volume loss after compensation	Girth Value (Method 1)	Girth Value (Method 2)	Deviation
0	0.00	0.00	246.86	246.65	0.21
5	1641.97	1.95	244.83	244.69	0.14
15	4608.26	1.67	238.55	238.47	0.08
25	7568.78	0.28	232.24	232.19	0.05

6. Conclusion

The existing methods of automatic girth measurement may bring obvious deviations by ignoring the elasticity of the limbs and the interactive deformation triggered by soft tape during manual measurement. To solve the problem, we exploit mass-spring model based volume preserving algorithm to describe the interactive limb deformation. Our method is tested with experiments and it has many potential applications.

Of course, the adopted models are assumed to have the equivalent elastic coefficients of the springs and the equivalent external forces imposed on the masses. However, if

realistic data of elastic coefficients and external forces are provided, our approach has the ability to simulate the anisotropic limb deformation by appointing the springs and the masses with their corresponding value.

7. Acknowledgment

The work was supported by National Basic Research Program of China (973 Program, No. 2011CB707904), National Natural Science Foundation of China (No. 60603079, 61070079, 71001066), Research Grants Council of Hong Kong (No. 613008).

References

- [1] Ding Y.H., Zhao J.H., Goonetilleke R.S., Xiong S.P., Yuan Z.Y., Zhang Y.Y., Long C.J., An Automatic Method for Measuring Foot Girths for Custom Footwear Using Local RBF Implicit Surfaces, *International Journal of Computer Integrated Manufacturing*, 23(2010), 574-583.
- [2] Xu C., Liu Y., Jiang Y., Pan Y., The design and implementation for personalized shoe last CAD system, *Journal of Computer-Aided Design & Computer Graphics*, 16(2004), 1437-1441.
- [3] Witana C.P., Xiong S.P., Zhao J.H., Goonetilleke R.S., Foot measurements from 3-dimensional scans: A comparison and evaluation of different methods, *International Journal of Industrial Ergonomics*, 36(2006), 789-807.
- [4] Zhao J.H., Xiong S.P., Bu Y.B., Goonetilleke R.S., Computerized girth determination for custom footwear manufacture, *Computers & Industrial Engineering*, 54(2008), 359-373.
- [5] Oomens C.W.J., Maenhout M., Oijen C.H.V., Drost M.R., Baaijens F.P., Finite element modeling of contracting skeletal muscle, *Philosophical Transactions of The Royal Society B-biological Sciences*, 358(2003), 1453-1460.
- [6] Nealen A., Matthias M., Richard K., Eddy B., Mark C., *Physically-based deformable models in computer graphics*, Computer Graphics Forum, 25(2005), 809-836.
- [7] De S., Lim Y.J., Manivannan M., Srinivasan M.A., Physically Realistic Virtual Surgery Using the Point-Associated Finite Field (PAFF) Approach, *Presence: Teleoperators and Virtual Environments*, 15(2006), 294-308.
- [8] Georgiia J., Westermann R., Mass-spring systems on the GPU, *Simulation Modeling Practice and Theory*, 13(2005), 693-702.
- [9] Hong M., Jung S., Choi M.H., Welch S.W.J., Fast Volume Preservation for a Mass-Spring System, *Computer Graphics and Applications*, 26(2006), 83-91.
- [10] Cormen T.H., Leiserson C.E., Rivest R.L., Stein C., Introduction to algorithm (Third Edition), *The MIT Press*, (2009).